ISBN: 978-3-95450-261-5 ISSN: 2673-7000 doi: 10.18429/JACoW-NAPAC2025-MOZN01

EXPLORATION OF ULTRA-HIGH DOSE RATE RADIOBIOLOGY WITH LASER-DRIVEN PROTONS AT BELLA

L. Obst-Huebl*, J. L. Inman, J. T. De Chant[1], K. Nakamura, A. J. Gonsalves, A. McIlvenny, J. Bin, B. Simmons, C. G. R. Geddes, C. B. Schroeder, C. Y. Ralston, J. van Tilborg, J.-H. Mao, S. Hakimi, S. Kidd, S. Subramanian, A. Snijders, E. Esarey
Lawrence Berkeley National Laboratory, Berkeley, CA, USA
B. Stassel, University of Michigan, Ann Arbor, MI, USA
C. A. J. Palmer, Queen's University Belfast, Belfast BT7 1NN, UK
L. Geulig, Ludwig-Maximilians-Universitaet Munich, Geschwister-Scholl-Platz 1, Munich, Germany
[1]also at Michigan State University, East Lansing, MI, USA

Content from this work may be used under the terms of the CC BY 4.0 licence (© 2025). Any distribution of this work must maintain attribution to the author(s), title of the work, publisher, and DOI.

INTRODUCTION

Laser-driven proton sources are of interest for various applications due to their ability to produce short proton bunches with high charge and low emittance. These sources can be used in biological studies investigating improvements to radiation cancer therapy. Recently, the differential sparing effect on normal tissues versus tumors using the delivery of high radiation doses, typically above 10 Gy, at extremely high dose rates, called FLASH effect, has received increasing attention [1, 2]. However, the molecular and cellular mechanisms underlying the sparing effect are not yet fully understood. To explore these mechanisms, we have fielded capabilities at the BELLA petawatt (PW) laser of Lawrence Berkeley National Laboratory (LBNL) to deliver laser-driven proton bunches at ultra-high instantaneous dose rate up to 10^8 Gy/s. This allowed us to investigate in vitro and in vivo the damage to normal tissue after exposure with laser-driven protons and prescribed doses of up to several 10 Gy [3, 4]. Reference measurements using 320 kV x-rays using an x-ray tube (X-RAD320) at clinical dose rates and soft x-rays with tunable dose rates at the Advanced Light Source of LBNL were established. Recent improvements to the laser-driven proton source, delivery beamline, and diagnostic suite have also enabled first peptide sample irradiations to explore the sparing effect on the molecular level. This paper gives an overview of capabilities available at LBNL for radiobiological research with ultra-high instantaneous dose rate laser-driven proton beams.

The general proton beamline setup at the BELLA PW is displayed in Figure 1 and consists of a target normal sheath acceleration (TNSA) proton source, magnetic proton transport optics, scatter foils for beam smoothing, apertures, a dipole, an exit window, and a biosample station with dosimetry diagnostics located in air. The dipole magnet is used to deflect protons downward onto the samples that are placed below the plane of the laser, to avoid exposure to electrons, x-rays and gamma-rays possibly also emitted by the proton source. More details on available proton sources, transport optics, beam diagnostics and sample stations are given in the following sections. The proton beam propagation through the beamline is modeled using a homemade MATLAB simulation code that combines the features of a traditional map code, through the integration of COSY INFINITY [5], with a Monte Carlo (MC) based radiation transport code [6]. Proton bunches accelerated via TNSA are ultra-short on the order of picoseconds at the source and then spread in time leading to nanosecond to few 10 ns bunch lengths when reaching the sample location. Time of flight analysis using the distance from TNSA source to sample combined with proton bunch propagation simulations and dose measurements result in a peak dose rate on the order of 10^7 to 10^8 Gy/s for irradiations with BELLA protons, depending on the configuration.

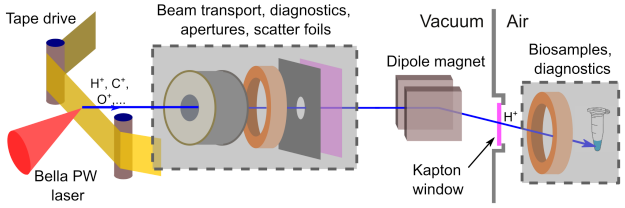

Figure 1: Laser-driven proton beamline for radiobiological studies at the BELLA PW laser of LBNL. Details of the general setup and options for beamline components in the grey placeholder boxes are given in the main text.

PROTON SOURCES

Proton bunches are accelerated via target normal sheath acceleration (TNSA) from a 13 µm thick kapton tape drive using the BELLA PW laser [7] at LBNL with up to 40 J laser pulse energy and down to 35 fs laser pulse length. The laser system and tape drive target allow for shot repetition rates up to 1 Hz, although irradiations were thus far conducted at shot rates of approximately one shot every 5 to 20 seconds. Two laser focusing geometries ("interaction points") are available that lead to different proton beam parameters, while both produce typical TNSA proton spectra with characteristic exponential shapes and cut-off energies. In the first (interaction point 1, iP1), the laser is focused using a 13.5 m focal length off-axis parabolic (OAP) mirror to a spot size

* lobsthuebl@lbl.gov

ISBN: 978-3-95450-261-5 ISSN: 2673-7000 doi: 10.18429/JACoW-NAPAC2025-MOZN01

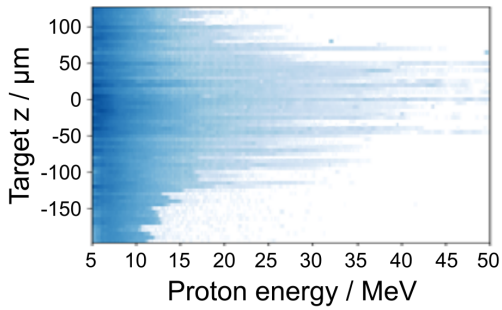

Figure 2: Proton beam spectra collected at BELLA PW iP2 at 0.2 Hz and scanning target position z along the laser focus. Each horizontal line is one proton spectrum, darker blue corresponds to higher particle numbers. Energies up to 45 MeV were observed at the best focus location for 22 J laser pulse energy on a 13 µm thick kapton tape target.

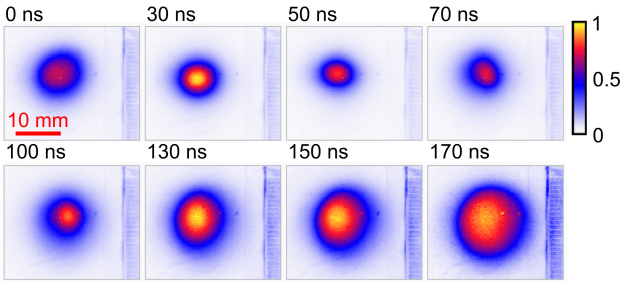

Figure 3: Active plasma lens discharge timing scan observing the proton beam spot (≈ 2 MeV proton energy) at the biosample location with a scintillator imaged to a CCD. The dipole was removed for this scan. Image color scales are individually normalized to peak signal. Here, longer discharge timing delay corresponds to an increasing current and, therefore, focusing field in the APL upon arrival of the TNSA proton bunch.

of 52 µm (full width at half maximum, FWHM), leading to high charge, low divergence proton beams with cut-off energies around 10 MeV [8]. In the second (iP2), a 500 mm focal length OAP focuses the beam to a spot size of 2.7 µm FWHM [9, 10], leading to higher energy proton acceleration up to 45 MeV for laser pulse energy of 22 J incident on the tape drive target (Fig. 2).

PROTON TRANSPORT SYSTEMS

Compact magnetic transport systems were established to deliver the TNSA proton bunches to a sample station located outside the vacuum chamber for quick sample replacements. The sample station is located approximately two meters downstream of the proton source. An active plasma lens (APL [11]) and a modular quadrupole doublet or quartet have been fielded as options for proton beam capture and transport. These are complemented by a selection of scatter foils and apertures for beam smoothing and collimation.
The APL provides a symmetric focusing field with a field strength that can be tuned with the discharge current (Fig. 3). In a previous implementation at iP1, the APL was used to deliver 2 MeV protons to cell samples [3]. A discharge current of 90 A was selected to create a smooth >10 mm diameter proton beam on the samples, delivering 1 Gy per laser shot. For this configuration, a transport efficiency of 0.2% was deduced (in vacuum for protons > 1.5 Mev), which is limited by the small ≈ 1 mm channel diameter of the APL.

A second beam transport option, featuring a modular set of permanent magnet quadrupoles (PMQs), was established to enable a higher capture efficiency using a larger bore (10-50 mm) while also lowering the system requirements (no discharge pulser needed). Two configurations were designed to collimate 10 MeV and 30 MeV proton beams, respectively. The first two PMQs were designed to transport a 10 MeV center energy. A second set of two PMQs could be added to the beam path to increase the overall focusing strength of the transport to transport a 30 MeV center energy. Both 10 and 30 MeV PMQ configurations were used in a previous implementation at the iP2 beamline to irradiate samples at greater penetration depths. A maximum transport improvement factor of 16 (5) was recorded for the 10 MeV (30 MeV) transport when comparing the proton charge at the sample site with versus without PMQs inserted [6, 12, 13]. Recently, the 10 MeV and 30 MeV configurations were implemented at BELLA iP2 to enable irradiations of murine ears in vivo and peptides in solution at a few Gy per shot [4].

All beamline transport options described here require accumulating laser shots to reach a prescribed dose of clinical relevance (10s of Gy) on each individual sample. Both laser and target system allow irradiations at 1 Hz, however, so far irradiations were conducted at repetition rates of 0.05 - 0.2 Hz, resulting in an average dose rate of a fraction of a Gy/s.

PROTON BEAM DIAGNOSTICS

Absolute doses for each irradiated sample are measured in situ with calibrated radiochromic films (RCF) attached to the front and/or back of each sample [14]. We have developed a film analysis protocol for cGy precision measurements, as well as Monte Carlo simulations that allow accounting for linear energy transfer effects in the RCF response [12]. In addition to that, integrating current transformers (ICTs) [15] and a scintillator-based beam monitor are used to record the proton charge and beam shape delivered to the samples with readout and analysis after every laser shot during sample irradiations. The linearity of the ICT measurement was confirmed in a comparison with a Faraday cup charge measurement. Correlation of the ICT-measured charge to film-measured doses at the ear location was established [16]. This allows for online dosimetry to guide sample irradiations and account for source fluctuations from shot to shot, which results in a more accurate targeting of the prescribed dose by adjusting the total number of LD proton bunches per sample.

Content from this work may be used under the terms of the CC BY 4.0 licence (© 2025). Any distribution of this work must maintain attribution to the author(s), title of the work, publisher, and DOI.

ISBN: 978-3-95450-261-5 ISSN: 2673-7000 doi: 10.18429/JACoW-NAPAC2025-MOZN01

© Content from this work may be used under the terms of the CC BY 4.0 licence (© 2025). Any distribution of this work must maintain attribution to the author(s), title of the work, publisher, and DOI.

The scintillator monitor placed at the end of the beamline records the two-dimensional (2D) spatial distribution of the proton beam after propagation through the whole system. With this dosimetry protocol we were able to conduct thin sample irradiations (250 µm) with 8 MeV protons at a total dose error of around 10 % [4].

BIOSAMPLE SYSTEMS

We designed and built low-cost and re-usable sample holders for irradiations. A motorized cell culture holder for in vitro irradiations allows for quick turnover between samples in cartridges with a circular beam entrance window of 1 cm diameter (Fig. 4 a). The maximum volume of cell culture media in each well is 270 µl, and when the holder is lifted in the upright position for proton irradiation, the media fills the adjacent cavity created underneath the window, thus clearing the path for the proton beam to enter and exit the chamber allowing for beam characterization downstream of the cell targets. A linear motorized stage was built to hold up to seven assembled cell cartridges to enable quick irradiation of subsequent samples without the need to enter the radiation shielded cave. For few MeV proton exposures, the samples were mounted at an angle of incidence of -135° to ensure cell culture media covered the cells (Fig. 4 a). Right before irradiation, each individual holder is remotely moved in position and lifted on a ramp to 0° to allow the cell culture media to fill the cavity leaving the cells with only a thin film of media and allowing for the proton beam to pass through the entrance mylar window, expose the cells, and pass through the exit mylar window onto RCF film for dose measurements. A similar pipeline was established for the irradiation of samples in centrifuge tubes (Fig. 4 b) with higher energy protons. Up to eight samples were irradiated in close succession. This assembly was first used for irradiations of peptides in 30 µl of solution. In both motorized sample pipelines, samples not currently irradiated were shielded from background radiation by introducing partial shielding of the assembly.

Figure 4 c) shows the holder commissioned for mouse ear irradiations in vivo. A soft padded ear clamp containing an 8 mm diameter beam entrance hole is fitted over the left ear of anesthetized mice and fixed in a pre-warmed aluminum base. A clear plexiglass top is fitted over the mouse and fixed in place. Shielding protects the remaining body of the mouse from radiation. The proton beam path before and after the ear is clear to allow for in situ film dosimetry. The design is aimed to minimize stress to the mice.

SOURCES FOR REFERENCE X-RAY MEASUREMENTS

Irradiation capabilities to study radiation damage to various samples were also established at a clinical dose rate x-ray tube (X-RAD320, Precision X-ray) and the Advanced Light Source (ALS) of LBNL. The X-RAD is routinely used by scientists for irradiations of cells and small animals and is

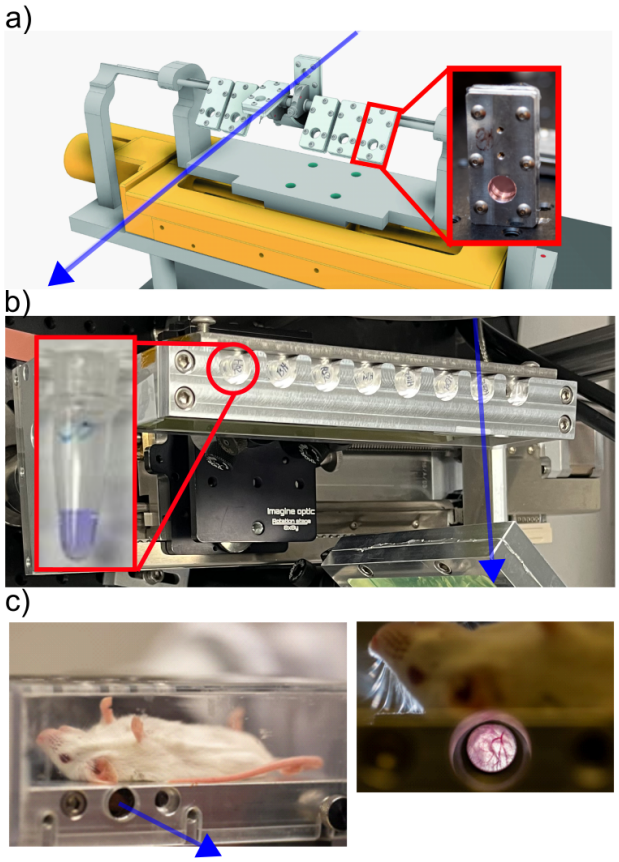

Figure 4: Biosample systems: a) pipeline for cell culture irradiations, b) pipeline for sample irradiations suspended in solution in centrifuge tubes, and c) mouse ear irradiation assembly for anesthetized mice.

frequently evaluated for its performance in dose homogeneity and absolute dose delivered to samples. Two beamlines at the ALS have been established to explore dose rate effects, delivering a broadband x-ray synchrotron spectrum at a high flux with critical energy 3.1 keV from a 1.3 T bending magnet. ALS's beamline 3.3.1 was used to irradiate peptide samples and study their oxidative damage via x-ray footprinting mass spectroscopy (XFMS) [17].

SUMMARY

Laser-driven proton source, beam delivery, and dose diagnostic capabilities were implemented in compact setups at the BELLA PW laser of LBNL for the exposure of biological samples to laser-driven proton beams. Sample insertion pipelines were developed to enable exposures of many samples with a quick turnaround. Reference x-ray exposure environments at varying dose rates were established at an x-ray tube and the Advanced Light Source at LBNL. These systems enable radiobiological research into the radiation damage induced by ultra-high instantaneous proton dose rates. They can also be used for the controlled exposure of other samples, such as to study defect engineering for emerging quantum devices [18].

ISBN: 978-3-95450-261-5 ISSN: 2673-7000 doi: 10.18429/JACoW-NAPAC2025-MOZN01

ACKNOWLEDGEMENTS

Work was supported by U.S. Department of Energy Office of Science (DOE-OS), FES, and HEP under DE-AC02-05CH11231, LaserNetUS, and LBNL's Laboratory Directed Research & Development (LDRD) Program. Work was partially conducted at the Advanced Light Source and the Molecular Foundry, which are supported by the DOE-OS under contract DE-AC02-05CH11231, and supported by the NIH R01 GM126218 and NIH P30 GM124169. J. D. was supported by DOE-OS, HEP under DE-SC0018362 and MSU. S. H. was supported by the DOE-FES Postdoctoral Research Program, administered by ORISE DE-SC0014664. B. S. was supported by the U.S. DOE-OS, WDTS, SCGSR program, also administered by ORISE.

REFERENCES

[1] V. Favaudon *et al.*, "Ultrahigh dose-rate FLASH irradiation increases the differential response between normal and tumor tissue in mice", *Sci. Transl. Med.*, vol. 6, no. 245, 2014. doi:10.1126/scitranslmed.3008973

[2] R. Schulte *et al.*, "Transformative technology for FLASH radiation therapy", *Appl. Sci.*, vol. 13, no. 8, p. 5021, 2023. doi:10.3390/app13085021

[3] J. Bin *et al.*, "A new platform for ultra-high dose rate radiobiological research using the BELLA PW laser proton beamline", *Sci. Rep.*, vol. 12, p. 1484, 2022. doi:10.1038/s41598-022-05181-3

[4] L. Obst-Huebl *et al.*, "Studying radiation damage to normal tissue in vivo with laser-driven protons at ultra-high instantaneous dose rate", 2025. in preparation.

[5] K. Makino and M. Berz, "COSY INFINITY version 9", *Nuclear Instruments and Methods in Physics Research Section A: Accelerators, Spectrometers, Detectors and Associated Equipment*, vol. 558, no. 1, pp. 346–350, 2006. doi:10.1016/j.nima.2005.11.109

[6] J. T. De Chant *et al.*, "Modeling and design of compact, permanent-magnet transport systems for highly divergent, broad energy spread laser-driven proton beams", *Phys. Rev. Accel. Beams*, vol. 28, no. 3, p. 033 501, 2025. doi:10.1103/PhysRevAccelBeams.28.033501

[7] K. Nakamura *et al.*, "Diagnostics, control and performance parameters for the BELLA high repetition rate petawatt class laser", *IEEE J. Quantum Electron.*, vol. 53, no. 4, p. 1 200 121, 2017. doi:10.1109/JQE.2017.2708601

[8] S. Steinke *et al.*, "Acceleration of high charge ion beams with achromatic divergence by petawatt laser pulses", *Phys. Rev. Accel. Beams*, vol. 23, no. 2, p. 021 302, 2020. doi:10.1103/PhysRevAccelBeams.23.021302

[9] L. Obst-Huebl *et al.*, "High power commissioning of BELLA iP2 up to 17 J", in *Proceedings Volume 12583, Applying Laser-driven Particle Acceleration III: Using Distinctive Energetic Particle and Photon Sources*, 2023. doi:10.1117/12.2669162

[10] S. Hakimi *et al.*, "Newly commissioned iP2 beamline of the BELLA PW facility for investigation of high intensity laser-solid interactions", in *2022 IEEE Advanced Accelerator Concepts Workshop (AAC22)*, pp. 1–5, 2022. doi:10.1109/AAC55212.2022.10822936

[11] J. V. Tilborg *et al.*, "Active plasma lensing for relativistic laser-plasma-accelerated electron beams", *Phys. Rev. Lett.*, vol. 115, no. October, p. 184 802, 2015. doi:10.1103/PhysRevLett.115.184802

[12] J. T. De Chant *et al.*, "Transport and dosimetry of laser-driven proton beams for radiobiology at the bella center", in *Proc. IPAC'24*, Nashville, TN, pp. 610–613, 2024. doi:10.18429/JACoW-IPAC2024-MOPR72

[13] J. T. De Chant *et al.*, "Design optimization of permanent-magnet based compact transport systems for laser-driven proton beams", in *2022 IEEE Advanced Accelerator Concepts Workshop (AAC22)*, pp. 1–6, 2022. doi:10.1109/AAC55212.2022.10822919

[14] J. H. Bin *et al.*, "Absolute calibration of GafChromic film for very high flux laser driven ion beams", *Rev. Sci. Instrum.*, vol. 90, p. 053 301, 2019. doi:10.1063/1.5086822

[15] K. Nakamura *et al.*, "Electron beam charge diagnostics for laser plasma accelerators", *Phys. Rev. Spec. Top. Accel Beams*, vol. 14, no. 6, pp. 1–11, 2011. doi:10.1103/PhysRevSTAB.14.062801

[16] L. D. Geulig *et al.*, "Online charge measurement for petawatt laser-driven ion acceleration", *Rev. Sci. Instrum.*, vol. 93, no. 10, p. 103 301, 2022. doi:10.1063/5.0096423

[17] S. Gupta *et al.*, "A novel platform for evaluating dose rate effects on oxidative damage to peptides: Toward a high-throughput method to characterize the mechanisms underlying the FLASH effect", *Radiat. Res.*, 2023. doi:10.1667/RADE-23-00131.1

[18] W. Redjem *et al.*, "Defect engineering of silicon with ion pulses from laser acceleration", *Commun. Mater.*, vol. 4, no. 22, 2023. doi:10.1038/s43246-023-00349-4

Content from this work may be used under the terms of the CC BY 4.0 licence (© 2025). Any distribution of this work must maintain attribution to the author(s), title of the work, publisher, and DOI.